J. Fluid Mech. (1989), *vol.* 207, *pp.* 1–28
Printed in Great Britain

On the flow between a porous rotating disk and a plane

By M. A. GOLDSHTIK AND N. I. JAVORSKY
Institute of Thermophysics, Siberian Branch of the USSR Academy of Sciences, Novosibirsk, 630090, Lavrentev Av. 1, USSR

(Received 8 April 1987 and in revised form 28 November 1988)

Axisymmetric flow of viscous incompressible fluid between a rotating porous disk and an impermeable fixed plane is investigated. It is shown that with injection and suction through a porous disk rotating with sufficiently large angular velocity there are many isolated steady self-similar solutions. In the case of suction through a fixed porous disk at a certain Reynolds number there exists bifurcation of the stable rotational regime of flow, implying a spontaneous break of the flow symmetry and an arbitrary rise of the fluid rotation within the framework of self-similarity. This unusual effect is discussed in detail, and the results of a relevant experiment are presented. Another unusual result is the existence of multicellular regimes consistent with suction, when the lift force acting on a rapidly rotating porous disk is anomalously large; in this case some of these regimes are stable relative to self-similar perturbations.

With sufficiently strong suction and rotation the stationary solution with large lift becomes unstable and the regime of self-oscillations arises. Diagrams of the possible stationary flow regimes have been constructed, and the stable ones have been identified. At the limit of vanishing viscosity we find, in the case of the suction, non-classical boundary layers on the solid surfaces characterized by a finite jump of the normal component of the velocity and unlimited tangential components. In this limit, in the interior flow region the singular non-viscous solution with an infinite velocity of rotation arises, while all limited non-singular admissible non-viscous solutions are not stable.

1. Introduction

Starting with the basic work by Kármán (1921), where a self-similar solution of the complete Navier–Stokes equations for flow above a rotating disk was examined, many papers have been devoted to the study of this and related solutions. In the fine reviews by Parter (1982) and Zandbergen & Dijkstra (1987) one can find the history of the problem and the current status of investigations into the problem of Kármán's self-similar flow between two impermeable disks. One of the major results of the analysis is the non-uniqueness of the exact self-similar solutions of the Navier–Stokes equations, where the additional solutions originate from the pairs which are not related by the bifurcational curve and their number increases infinitely with the growth of Reynolds number. Newly arising solutions are characterized, as a rule, by a multicellular structure (Mellor, Chapple & Stokes 1968). However, unicellular solutions can also exhibit non-uniqueness. This non-uniqueness of the flow regimes between impermeable disks has been experimentally verified (Mellor *et al.* 1968; Nguyen, Ribault & Florent 1975; Dijkstra & Heijst 1983; Szeri *et al.* 1983*a*) and it has been found that for each particular experimental installation only one regime of the flow exists, though it can be of different types at different installations. Experiments have shown considerable influence of boundary effects, extending approximately to half the disk radius. Therefore some non-self-similar problems for the flow between disks of finite size have been examined by Adams & Szeri (1982), Dijkstra & Heijst (1983) and Brady & Durlofsky (1986).

Numerical solutions of these problems have shown that in the non-self-similar formulation there is only one solution and it is in good agreement with the results of experiments (Dijkstra & Heijst 1983). Hence one can draw the conclusion that the boundary conditions on the cylindrical surface limiting the disks are the determining ones for the choice of one of the possible self-similar solutions. However, the question of whether there exist such external boundary conditions under which stable multicellular regimes are realized is left open. The stability of these flows is discussed in the review by Zandbergen & Dijkstra (1987). In this connection the work by Szeri *et al.* (1983*b*) should also be mentioned. A considerable number of papers (see Parter 1982; Zandbergen & Dijkstra 1987) is devoted to the numerical investigation of the problem in which a great number of solutions has been found. Determination of the entire set of solutions with arbitrary given angular velocities meets pronounced computational difficulties. They are attributed to the fact that all multicellular solutions do not arise due to the bifurcation of the unicellular solution (Rasmussen 1973) and they are isolated, that is not typical, in general, for hydrodynamics.

In the work by Batchelor (1951) Kármán's self-similar solutions were extended to flows above a rotating impermeable disk with prescribed fluid rotation at infinity and flows between infinite rotating porous disks with given uniform suction or injection. The presence of additional parameters of injection or suction complicates significantly the problem. Thus, the analysis of more complicated flows between rotating disks, given uniform injection or suction, by Stuart (1954), Dorfmann (1966), Elkouh (1968, 1970), Evans (1969), Rasmussen (1970), Kuiken (1971), Jawa (1971), Ockendon (1972), Narajana & Rudraiah (1972), Wang (1976), Wilson & Schryer (1978), Wang & Watson (1979), Elcrat (1980), Coselskaya & Lumkis (1980), Petrovskaya (1982) have, for the most part, been done without any connection with the problem of the non-uniqueness of the Navier–Stokes equation solutions. However, as will be shown here, the presence of sufficiently large suction in the problem with fixed disks results in non-uniqueness of a new type, namely bifurcation of rotation that has a non-trivial physical interpretation in the form of a spontaneous rise in the flow rotation.

A problem arises concerning the description of the entire set of solutions for self-similar Kármán flows depending on the values of the angular velocities of the disks and the velocity of uniform injection or suction. We believe that this problem is solved to some extent in the present work by reducing the boundary problem of the flow between a rotating porous disk and a plane to an initial-value problem with a biparametrical family of solutions. Such a representation turns out to be well-posed and permits, in principle, the determination of the whole family of solutions with the help of a simple algorithm. Since numerical calculations show that there exists a multiplicity of isolated solutions, numerous attempts have been made in rigorous mathematical analysis of the flow between the disks to prove or disprove the existence of such solutions. For the problem with impermeable disks a sufficiently complete representation of the corresponding results can be found in the reviews mentioned above. For the problem with injection or suction, only some individual results are known. Elcrat (1976) has proved the theorem of existence and uniqueness for non-rotational fluid motion between fixed porous disks with arbitrary uniform injection or suction, but there are no accurate results dealing with the self-similar flow between rotating disks with uniform injection or suction. Nevertheless, non-viscous analysis permits the determination of some features of the solution behaviour in this case. Section 3 considers a general form of non-viscous vortex-type solution, which permits the determination, in the limit of vanishing viscosities, of a finite number of solutions at non-zero suction or injection, whereas in the case of impermeable disks a number of solutions is at least countably infinite (Parter 1982). At $\nu \to 0$ the non-viscous analysis can be supplemented by numerical investigation, with the help of which the regions of existence of various types of solution have been determined on the basis of a special algorithm. In the present paper, to make the solution of the self-similar problem of the flow between two infinite porous disks more tractable for analysis, as a whole, the problem of the fluid flow between a rotating porous disk and a fixed plane is examined alone. This problem models qualitatively the flow under a body on an air cushion and therefore it can be of interest from a practival viewpoint. In this case the flow is defined by two parameters: Reynolds number $R = Vh/\nu$ based on the injection or suction velocity V; and the twisting parameter $K = \Omega h/V$, where h is a disk-to-disk distance and Ω is the angular velocity of the porous disk. The choice of K instead of the traditionally used rotational Reynolds number $R_\omega = \Omega h^2/\nu$ or $Ek = 1/R_\omega$ is more convenient for the interpretation of data related to a disk on an air cushion with rotation, since K characterizes the geometry of the device twisting the flow only (Goldshtik 1981). In the general case we need two more parameters: the ratio of disk angular velocities and the ratio of suction or injection velocities.

2. Formulation

Let $z = 0$ correspond to a fixed impermeable plane and $z = h$ to a rotating porous disk through which uniform injection or suction occurs.

The Navier–Stokes equations for axisymmetric motion of incompressible fluid are written in the form (notation is conventional)

$$\frac{\partial v_r}{\partial t} + v_r \frac{\partial v_r}{\partial r} + v_z \frac{\partial v_r}{\partial z} - \frac{\partial_\phi^2}{r} = -\frac{1}{\rho}\frac{\partial p}{\partial r} + \nu\left(\frac{\partial}{\partial r}\frac{1}{r}\frac{\partial r\, v_r}{\partial r} + \frac{\partial^2 v_z}{\partial z^2}\right), \tag{2.1}$$

$$\frac{\partial r\, v_\phi}{\partial t} + v_r \frac{\partial r\, v_\phi}{\partial r} + v_z \frac{\partial r\, v_\phi}{\partial z} = \nu\left(r\frac{\partial}{\partial r}\frac{1}{r}\frac{\partial r\, v_\phi}{\partial r} + \frac{\partial^2 r\, v_\phi}{\partial z^2}\right), \tag{2.2}$$

$$\frac{\partial v_z}{\partial z} + v_r \frac{\partial v_z}{\partial r} + v_z \frac{\partial v_z}{\partial z} = -\frac{1}{\rho}\frac{\partial p}{\partial z} + \nu\left(\frac{1}{r}\frac{\partial}{\partial r} r \frac{\partial v_z}{\partial r} + \frac{\partial^2 v_z}{\partial z^2}\right), \tag{2.3}$$

$$\frac{\partial r\, v_r}{\partial r} + \frac{\partial r\, v_z}{\partial z} = 0. \tag{2.4}$$

We shall seek the self-similar Kármán solution in the form

$$v_z = v_z(z,t), \quad v_\phi = v_\phi(r,z,t) = r\omega(z,t). \tag{2.5}$$

According to (2.4) we have $v_r = -\frac{1}{2} r v_z'$, where the prime denotes differentiation with respect to z. According to (2.1) $\partial p/\partial r = \rho r F(z,t)$, then according to (2.3) $\partial p/\partial z = \rho f(z,t)$, so that $\partial^2 p/\partial r\,\partial z = 0$. Hence, $F' = 0$ and $F = F(t)$. For further calculations it is convenient to put $F = -\frac{1}{2}\alpha^2\delta$, where $\alpha = \alpha(t)$ is the value to be determined, and $\delta = \pm 1$. Thus we obtain

$$\frac{1}{\rho}\frac{\partial p}{\partial r} = -\tfrac{1}{2}\alpha^2\delta r. \tag{2.6}$$

Substitution of these results in (2.1) yields the equation

$$\frac{\partial v_z'}{\partial t} = \nu v_z''' + \tfrac{1}{2}v_z'^2 - v_z v_z'' - 2\omega^2 - \alpha^2\delta. \tag{2.7}$$

Differentiation of this equation with respect to z allows the elimination of the unknown α:

$$\frac{\partial v_z''}{\partial t} = \nu v_z^{\mathrm{IV}} - v_z v_z''' - 4\omega\omega'. \tag{2.8}$$

Similarly, proceeding from (2.2) we obtain the equation

$$\frac{\partial \omega}{\partial t} = \nu\omega'' - v_z\omega' + v_z'\omega. \tag{2.9}$$

For the system of equations (2.8), (2.9) no-slip boundary conditions, except initial ones, are prescribed:

$$\left.\begin{aligned} v_z(0) &= 0, \quad v_z'(0) = 0, \quad \omega(0) = 0, \\ v_z(h) &= V, \quad v_z'(h) = 0, \quad \omega(h) = \Omega. \end{aligned}\right\} \tag{2.10}$$

The number of conditions (2.10) corresponds to the order of system (2.8), (2.9). In the present paper it is the stationary problem that is basically under study, in which $\partial v_z/\partial t = 0, \partial\omega/\partial t = 0$. After making it non-dimensional two independent physical parameters arise in the stationary case: Reynolds number $R = Vh/\nu$; and the magnitude of flow twisting $K = \Omega h/V$. Even in the stationary case the nonlinear boundary problem (2.8)–(2.10) is a difficult one for both analytical study and the numerical solution. To study the whole set of possible solutions it is expedient to reduce the stationary boundary-value problem to a Cauchy problem. It is convenient to introduce new variables, putting

$$v_z = (\alpha\nu)^{\frac{1}{2}}W(x), \quad v_r = -\tfrac{1}{2}\alpha r W'(x), \quad v_\phi = \alpha r\gamma(x); \quad x = \left(\frac{\alpha}{\nu}\right)^{\frac{1}{2}} z. \tag{2.11}$$

Then the stationary equations (2.7), (2.9) can be written in a form containing no parameters:

$$W''' = WW'' - \tfrac{1}{2}W'^2 + 2\gamma^2 + \delta, \tag{2.12}$$

$$\gamma'' = W\gamma' - \gamma W', \tag{2.13}$$

where the prime denotes differentiation with respect to x. Note that according to (2.6) the variable α has dimension s^{-1}, so that the variables x, W and γ are non-dimensional. An auxiliary initial-value problem is formulated at $x = 0$:

$$W = 0, \quad W' = 0, \quad W'' = P, \quad \gamma = 0, \quad \gamma' = Q. \tag{2.14}$$

It contains only two parameters, P and Q, which allows the complete investigation of the problem to be carried out separately for $\delta = 1$ and $\delta = -1$. Changing the parameters $-\infty \leqslant P \leqslant \infty$, $-\infty \leqslant Q \leqslant \infty$ one can obtain the whole set of solutions of the initial boundary-value problem with all admissible values of R and K.

The initial-value problem (2.12)–(2.14) is related to the initial boundary-value problem by integrating the system of equations for a value $x = x_m$ such that the penultimate condition (2.10) is satisfied, i.e. $W'(x_m) = 0$. In this case the variables $W_m = W(x_m)$ and $\gamma_m = \gamma(x_m)$ are determined. Using (2.11) they can be readily related to the initial parameters of the problem, R and K. Having previously determined the variable $\alpha = x_m^2 \nu/h^2$, we have

$$R = W_m x_m, \quad K = \gamma_m x_m / W_m. \tag{2.15}$$

The initial-value problem (2.12)–(2.14) has a unique analytical solution for every set of P, Q, δ, to which a single, several or no values $x_m > 0$ can correspond, where $W' = 0$.

We can readily calculate the force of 'flow–wall' interaction, if we use the expression for the tensor of impulse flux density:

$$\Pi_{ij} = \rho\left[v_i v_j - \nu\left(\frac{\partial v_i}{\partial x_j} + \frac{\partial v_j}{\partial x_i}\right)\right] + p\delta_{ij}.$$

Proceeding from (2.3) for the stationary case it is not difficult to obtain

$$\frac{p}{\rho} = \frac{p_0}{\rho} + \nu\frac{\partial v_z}{\partial z} - \frac{v_z^2}{2} - \frac{\alpha^2\delta}{4}r^2, \quad p_0 = \text{const.}$$

Then taking account of (2.11) and the equality $\alpha = \nu x_m^2/h^2$ we find

$$\Pi_{zz} = p_0 - \frac{\rho\nu^2 r^2}{4h^4}\delta x_m^4 + \frac{\rho\nu^2}{h^2}x_m^2(\tfrac{1}{2}W^2 - W').$$

When calculating the force acting on a disk of large radius L the last component of this expression can be neglected. Therefore, choosing the constant p_0 such that $p(L) = 0$ we obtain the following expression for the lifting force acting on the porous disk:

$$\mathscr{F} = 2\pi\int_0^L \Pi_{zz}\, r\, \mathrm{d}r|_{z=h} = \tfrac{1}{8}\pi\rho\nu^2\left(\frac{L}{h}\right)^4 x_m^4\,\delta\left[1 + O\left(\frac{h^2}{L^2}\right)\right]. \tag{2.16}$$

For the force moment on any wall we have

$$M = 2\pi\int_0^L \Pi_{z\phi}\, r^2\, \mathrm{d}r|_{z=0,h} = \tfrac{1}{2}\pi\rho\nu^2 L\left(\frac{L}{h}\right)^3 (W\gamma - \gamma')|_{x=0,x_m}. \tag{2.17}$$

It is simpler to solve the outlined program numerically, leaving the analytical study for limiting cases only.

3. Physical analysis

First, let us consider the variable δ, which according to (2.6) determines unambiguously the sign of the radial pressure gradient. The zone of increased pressure near the flow symmetry axis corresponds to the value $\delta = 1$ and the rarefaction zone corresponds to $\delta = -1$.

A rigorous asymptotic analysis of the problem presents considerable difficulties and is hardly justified. Nevertheless, for a preliminary study of the qualitative solution behaviour it is necessary to consider the limiting cases $\nu \to \infty$ and $\nu \to 0$. At the physical level we proceed from the formulation of the stationary $(\partial/\partial t \equiv 0)$ problem (2.8)–(2.10).

In the case $\nu \to \infty$ after eliminating nonlinear terms we obtain

$$\nu v_z''' = \alpha^2\delta, \quad \omega'' = 0.$$

The solution satisfying the conditions (2.10) has the form

$$v_z = V\left[3\left(\frac{z}{h}\right)^2 - 2\left(\frac{z}{h}\right)^2\right], \quad \omega = \Omega\frac{z}{h}; \quad V = -\frac{\alpha^2\delta}{12\nu}h. \tag{3.1}$$

The last relation shows that $\delta = 1$ corresponds to injection ($V < 0$) and $\delta = -1$ corresponds to suction. The relation between the parameters R, K and P, Q is of the form

$$R = -\tfrac{4}{3}P^4\delta, \quad K = 6Q/P. \tag{3.2}$$

Without any loss of generality one can assume that $\Omega > 0$ and $Q > 0$. Then the sign of P coincides with the sign of V, so that in the case of suction $P > 0$, and injection $P < 0$. All these properties are in agreement with common sense: at injection an increased-pressure zone is formed under the disk, and at suction vice versa – the rarefaction zone is formed.

Let us now consider a stationary 'non-viscous' solution, putting $\nu = 0$ into (2.7) and (2.9). In this case (2.9) is easy to integrate (Dijkstra 1980):

$$\omega = \tfrac{1}{2}Av_z, \quad A = \text{const.} \tag{3.3}$$

Taking into account (3.3), (2.7) takes the form

$$v_z v_z'' - \tfrac{1}{2}v_z'^2 + \tfrac{1}{2}A^2 v_z'^2 + \alpha^2\delta = 0. \tag{3.4}$$

It is also easy to obtain a general integral of (3.4):

$$v_z = \frac{B}{A} + \frac{(B^2 + 2\alpha^2\delta)^{\frac{1}{2}}}{A}\sin A(z+\beta), \tag{3.5}$$

where B, β are arbitrary constants. From (3.4) or (3.5) it follows that it is necessary to have $\delta = +1$ to make v_z vanish. At $\delta = -1$, as one can see directly from (3.4), there is a particular solution $v_z = \text{const}$ corresponding to solid-body rotation with $\omega^2 = \frac{1}{2}\alpha^2$.

Equations (3.3) and (3.5) describe a four-parameter class of vortex motion for an ideal fluid. By choosing the parameters A, B, α, β one can, in principle, satisfy four out of the six conditions (2.10). Which particular conditions should be taken to obtain the final result follows from the specific physical formulation of the problem. One of the major physical requirements in this case is the absence of boundary layers in sections where fluid flows in (Judovich 1962). However, one should bear in mind that in the process of approaching the limit $\nu \to 0$, physical boundary conditions (2.10) can be 'erased' as a result of boundary-layer formation. Analysis and numerical calculations show that this really does occur and in this case not only no-slip conditions but also impermeable conditions can be 'erased'. In this case the parameters of (3.5) should be determined by detailed treatment of the approach to the limit in the total viscous solution.

A sufficiently complete analysis of the problem in the case of impermeable disks has been expounded in the reviews by Parter (1982) and Zandbergen & Dijkstra (1987). In the case of rotating porous disks with uniform injection or suction the situation changes qualitatively. First, note that the non-viscous solution (3.3), (3.5) can satisfy five of the six conditions in (2.10). In the case of injection the solution is unique and has the form

$$v_z = \frac{V \sin k \frac{z}{h} \sin k\left(2-\frac{z}{h}\right)}{\sin^2 k}, \quad V < 0; \tag{3.6}$$

$$\omega = \frac{k}{h} v_z, \quad k = \tfrac{1}{2}Ah = \frac{\Omega h}{V}. \tag{3.7}$$

Of all the conditions (2.10), the only one not satisfied by (3.6) is the no-slip condition $v_z'(0) = 0$. Hence, it is natural to assume that when $\nu \to 0$, the classical boundary layer occurs for an impermeable plate at $z = 0$ under the viscous solution. When the case of inflow is considered, a boundary layer at the permeable disk should be absent, as assured by the fulfilment of the condition $v_z'(h) = 0$ for (3.6).

The solution (3.6) is sign-dependent only at $K \leqslant \frac{1}{2}\pi$. It is remarkable that at $K = \frac{1}{2}\pi$ the no-slip condition $v_z'(0) = 0$ is also fulfilled, so that in this case (3.6) is obviously an exact limit for the viscous solution when $\nu \to 0$. It should be noted that $\alpha = 0$ for this solution, i.e. $\partial p/\partial r = 0$ according to (2.6). This is seen from the relationship

$$\alpha^2 \delta = 2\left(\frac{V}{h}\right)^2 K^2 \cot^2 K, \tag{3.8}$$

obtained by substitution of (3.6), (3.7) into (3.4). If $K > \frac{1}{2}\pi$, (3.6) changes sign and describes a multicellular regime. However, analytical solution (3.6) in the neighbourhood of the point z_0, where $v_z(z_0) = 0$ is not appropriate. This follows directly from stationary equation (2.9):

$$\nu \omega'' = v_z \omega' - v_z' \omega. \tag{3.9}$$

Both components of the right-hand side of (3.9) are zero at first order for the analytical solution (3.6), whereas $\omega''(z_0) \neq 0$. Hence, the viscous term cannot be neglected in the neighbourhood of the point z_0. This means that the limiting solution at $\nu \to 0$ should be constructed as a solution composed of non-viscous ones which are different on different sides of the point z_0, where the internal boundary layer arises. This situation is the same as in the theory of hydrodynamical stability when a critical layer arises (Lin Tsa-Tsao 1958) as a result of the degeneration of the differential equation ($v_z(z_0) = 0$ in (3.4)). It is most natural to construct the composite solution on the basis of physical considerations, assuming that $\alpha = 0$ for $K > \frac{1}{2}\pi$. According to (3.8) the increase of the value K from zero to $\frac{1}{2}\pi$ results in the decrease of pressure gradient $\alpha^2\delta$ up to zero. A further increase of rotation, according to (3.8), should cause a pressure increase near the axis, which seems to be physically inappropriate. But if $\alpha = 0$ at $K > \frac{1}{2}\pi$ then in the zone $z_0 < z < h$ the solution is of the form

$$v_z = V \sin^2 K \frac{z - z_0}{h}, \quad \omega = \frac{K}{h} v_z; \quad z_0 = h\left(1 - \frac{\pi}{2K}\right). \tag{3.10}$$

Solution (3.10) is characterized by the fact that, at $z = z_0$, not only $v_z = \omega = 0$ but also $v_z' = 0$, i.e. the fluid is at rest at this point. In such case the stationary fluid is permissible over the entire zone $0 \leqslant z \leqslant z_0$. Such a possibility for a composite solution is not unique. For instance, in the zone $0 \leqslant z \leqslant z_0$, 'eigen' motion is admitted with the velocity field

$$v_z = C \sin^2 \frac{\pi z}{z_0}, \quad \omega = \frac{\pi}{z_0} v_z. \tag{3.11}$$

where C is an arbitrary constant.

It should be noted that 'eigen' solution (3.11) is not the only possible non-trivial solution in the region $0 \leqslant z \leqslant z_0$. This region can be divided into any number of subregions, so that in every zone obtained there occurs 'eigen' motion of the type (3.11).

According to Parter (1982) solutions of the form (3.10), (3.11) are limiting ones for the viscous solution when $\nu \rightarrow 0$. The magnitude of C in (3.11) can be obtained by the method of matched asymptotics (Dijkstra 1980) which, in the present case, is reduced to the following. In (3.9), $v_z = A(z-z_0)^2$ is assumed, where $A < 0$ in the injection case under consideration. The solution of linear equation (3.9) is obtained analytically in the form of Kummer's function $U(-\frac{2}{3}, \frac{2}{3}, A(z-z_0)^3/3\nu)$ which has different asymptotical behaviour for $z \rightarrow +\infty$ and $z \rightarrow -\infty$, so that

$$\omega''(+\infty)/\omega''(-\infty) = -2. \tag{3.12}$$

(We note that in the work by Dijkstra (1980) this ratio is $-\frac{1}{2}$ as the case $A > 0$ is considered.) It stands to reason that (3.12) is valid only under the condition that motion can occur on both sides of the boundary $z = z_0$. It is clear from (3.12) that the fluid rotation changes to an opposite one on crossing the boundary z_0. This analysis shows that matched solutions have continuous v_z, v_z', v_z'', ω, ω' at $z = z_0$, but higher derivatives have a discontinuity. Discontinuity of the function ω'' at the point z_0, under the condition of continuity v_z'', predetermines the jump of the constant k in the relationship $\omega = kv_z/h$. Let $k = k_1$ in the region $z \leqslant z_0$, then in accordance with (3.12) we have $k_1/K = -\frac{1}{2}$. Writing the conditions of continuity in terms of the composite non-viscous solution (3.10) and the 'eigen' solution

$$v_z = V_1 \sin^2 k_1 \frac{z-z_1}{h}, \quad \omega = \frac{k_1}{h} v_z; \quad z_1 = z_0 - \frac{h\pi}{|k_1|}, \tag{3.13}$$

determined in a certain region $z_1 \leqslant z \leqslant z_0$, we obtain relationships

$$k_1 = -\tfrac{1}{2}K, \quad k_1^2 V_1 = K^2 V. \tag{3.14}$$

These relationships restrict an arbitrary choice of subregions with appropriate 'eigen' solutions; in particular, we have $z_1 = h(1 - 5\pi/2K)$, comparing (3.14) and (3.13) with due account of (3.10). Therefore a proper circulating zone can arise only at $K > \frac{5}{2}\pi$, since $z_1 > 0$ should hold. If $\frac{1}{2}\pi < K < \frac{5}{2}\pi$, then in the region $z \leqslant z_0$ the fluid is at rest. Notice that for $K > \frac{5}{2}\pi$ the solution with $v_z \equiv 0$ at $z \leqslant z_0$ is permissible, so that there is non-uniqueness of limiting non-viscous regimes. The number of similar solutions increases with the growth of K. Generalizing (3.14), one can write

$$k_0 = K, \quad k_i = -\tfrac{1}{2}k_{i-1}, \quad k_i^2 V_i = k_{i-1}^2 V_{i-1}, \tag{3.15}$$

where $i = 1, 2, \ldots$ denotes each internal boundary layer, counted out from the rotating porous disk. One can easily see that the location of the $(i+1)$th internal boundary layer is defined by the expression

$$z_i = z_{i-1} - h\frac{\pi}{|k_i|}. \tag{3.16}$$

By virtue of the limitation $z_i \geqslant 0$, the number of additional zones with 'eigen' motion is determined by the value K. Thus, according to (3.15), (3.16), in the region of parameter variation

$$2\pi(2^{n+1}-1) > K-\tfrac{1}{2}\pi \geqslant 2\pi(2^n-1), \quad n = 1,2,3,\ldots$$

n additional zones are possible. And in the neighbourhood of the plane $z = 0$, if the eigen zone does not occupy it, the rest condition should apply. Therefore the number of possible solutions is $n+1$. Take note that the number of solutions increases infinitely for impermeable disks when $K \to \infty$.

In the case of suction ($V > 0$) solutions (3.10), (3.13) are also permissible. However, the method of matched asymptotics which is applied in the neighbourhood of a rotating porous disk $z = h$ yields $k_0 = 0$ under the condition of continuity for normal velocity v_z. Let the velocity have the form

$$v_z = V+O((h-z)^2), \quad v_r = O(h-z)$$

in the neighbourhood close to the point $z = h$.

From (3.9) we find

$$\omega = \Omega\, \mathrm{e}^{V(z-h)/\nu}[1+O(h-z)].$$

This relationship characterizes an equilibrium between diffusion of rotation propagating from the end $z = h$ into the depth of fluid and convection due to the suction. In the limit when $\nu \to 0$, $\omega \to 0$ for all $z < h$. In this case the solution in the internal region of the flow is of the form

$$v_z = V\frac{z^2}{h^2}, \quad \omega \equiv 0, \quad 0 \leqslant z < h, \tag{3.17}$$

but at $z = h$ a thin boundary layer exists. However, in the presence of suction ($\delta = -1$), as already mentioned, there is a particular non-viscous solution v_z = const. It cannot satisfy the no-slip condition on the plane, but the Navier–Stokes equations (2.1)–(2.4) admit the existence of a non-classical boundary layer, on the external boundary of which the normal velocity $v_z \sim 1$ is given. For such a boundary layer one can obtain in a standard manner the estimates

$$\delta_v \sim \nu, \quad v_r \sim 1/\nu, \quad v_\phi \sim 1/\nu, \quad \alpha \sim 1/\nu \tag{3.18}$$

where δ_v is the thickness of the boundary layer. Estimates (3.18) stipulate the existence of intensive boundary flows with large tangent velocities. In particular, the entire radial flow is concentrated near the walls $z = 0$ and $z = h$. These boundary layers are consistent with the particular solution v_z = const, therefore a non-viscous limit is permissible

$$v_z = \text{const}, \quad \omega^2 = -\tfrac{1}{2}\alpha^2\delta = \text{const}, \quad \delta = -1, \tag{3.19}$$

and besides (3.17) there are solutions of the form

$$\omega_1 = \alpha/\sqrt{2}, \quad \omega_2 = -\alpha/\sqrt{2}, \quad \alpha \sim 1/\nu. \tag{3.20}$$

Solutions (3.19), (3.20) are unusual in two aspects. First, they are characterized by discontinuities of normal velocity v_z at the boundaries $z = 0$ and $z = h$. Secondly, internal rotation rises to any value when $\nu \to 0$, irrespective of the given value $\omega(h) = \Omega$, testifying to generation of rotation inside the flow region. But then one can expect such generation for $\Omega = 0$ too. If this is so, a Reynolds number R_{cr} may be found at which similar self-rotation arises for the first time, since (3.1) is unique for small R. As is well known (Arnol'd 1978), the phenomenon of direct bifurcation is accompanied by the loss of initial regime stability. Hence, the energy method is applicable to find the supposed point of bifurcation.

Let us consider the problem of suction through the upper disk at rest for arbitrary R. As is known (Elcrat 1976), this problem has a unique solution on the assumption that $v_\phi \equiv 0$. Multiplying the non-stationary equation (2.9) for the velocity component ϕ by ω and integrating with respect to z from 0 to h we obtain the energy equality

$$\frac{\partial}{\partial t}\int_0^h \tfrac{1}{2}\omega^2\,dz = -\nu\int_0^h\left(\frac{\partial\omega}{\partial z}\right)^2 dz + \frac{3}{2}\int_0^h \frac{\partial v_z}{\partial z}\omega^2\,dz, \tag{3.21}$$

where integration has been performed by parts taking into account the boundary no-slip conditions $\omega(t,0) = \omega(t,h) = 0$. If the right-hand side of (3.21) becomes positive when ν decreases, then the initial motion loses stability with respect to the rotation. This will occur for certain if the last term is positive and the first one vanishes when $\nu \to 0$. For an estimation of the stability loss it is sufficient to restrict attention to the case of small ω when the basic flow is described by a solution without rotation, which changes to (3.17) with the formation of an ordinary boundary layer at the upper wall when $\nu < 0$. Therefore, at small viscosities the first term on the right-hand side of (3.21) can be evaluated using traditional estimates of boundary-layer theory:

$$\nu\int_0^h\left(\frac{\partial\omega}{\partial z}\right)^2 dz \sim \nu\frac{\omega_0^2}{\delta_\omega^2}\delta_\omega \sim \omega_0^{\frac{5}{2}}\nu^{\frac{1}{2}}, \tag{3.22}$$

where $\delta_\omega \sim (\nu/\omega_0)^{\frac{1}{2}}$ is the thickness of the boundary layer with respect to velocity v_ϕ, and ω_0 is a certain characteristic angular velocity of rotation. Thus, the contribution of this integral is negligibly small when $\nu \to 0$.

Using the results obtained by Elcrat (1976), one can show that the solution of the problem without rotation ($\omega \equiv 0$) is monotonic: for suction $\partial v_z/\partial z > 0$, and for injection $\partial v_z/\partial z < 0$ for $0 < z < h$ and all values of viscosity ν. In particular, in the case of suction the non-viscous limit has the form of (3.17). Therefore, the last term on the right-hand side of (3.21) is positive.

Thus, the solution with suction and without rotation at sufficiently large Reynolds numbers R is unstable with respect to rotational motion. In the case of injection the damping of rotation follows from (3.21) for all ν.

As has already been stated, rotational instability arises with the growth of Reynolds number at suction through the upper disk and indicates a bifurcation of the stationary solution. Proceeding from (3.21) one can estimate the Reynolds number at which this bifurcation takes place. For this purpose we use a well-known Courant's inequality (Rectoris 1985)

$$\int_0^h\left(\frac{\partial\omega}{\partial z}\right)^2 dz \geqslant \frac{\pi^2}{h^2}\int_0^h \omega^2\,dz \quad (\omega(0) = \omega(h) = 0)$$

as an estimate, where the sign $\geqslant$ is replaced by $\sim$. Let us evaluate the second integral on the right-hand side of (3.21), taking into account that the variable $\partial v_z/\partial z$ does not change the sign, in the following form:

$$\int_0^h \frac{\partial v_z}{\partial z}\omega^2\,dz \sim \frac{V}{h}\int_0^h \omega^2\,dz,$$

where V is the velocity of suction through the upper disk. Hence, we shall find that the critical Reynolds number at which the right-hand side of (3.21) goes to zero has the value

$$R_{\text{crit}} \sim \tfrac{2}{3}\pi^2 \approx 6.5. \tag{3.23}$$

It turns out that, in spite of the roughness of the estimate, an accurate calculation of the Reynolds number at which the rotation bifurcation occurs results in a magnitude close to the value in (3.23).

Apart from the results obtained, (3.21) may be used to justify the existence of the particular stationary solutions (3.19), (3.20) with non-classical boundary layers. In fact, for such solutions both terms on the right-hand side of (3.21) have the same order for $\nu \rightarrow 0$,

$$\nu \int_0^h \left(\frac{\partial \omega}{\partial z}\right)^2 \mathrm{d}z \sim \int_0^h \frac{\partial v_z}{\partial z} \omega^2 \,\mathrm{d}z \sim \frac{1}{\nu^2},$$

that is a necessary condition for the existence of a stationary regime. Numerical investigation into the evolution of self-similar solutions confirms the existence of stable particular stationary solutions (see §5).

4. Results of numerical calculations

In accordance with the programme set out in §2, the initial-value problem (2.12)–(2.14) will now be solved. Let us consider by way of example how integral curves $W'(x)$ behave at the fixed values of $P = 0.5$, $\delta = -1$ and various Q. Calculation data are presented in figure 1 where four integral curves are plotted. To solve the boundary-value problem it is necessary to search for the values $x = x_m$ so that $W'(x_m) = 0$. From figure 1 we see that all curves go finally to $+\infty$; that it happens at finite x_∞ is typical for nonlinear equations. As numerous calculations have shown, this property 'to attract' the solutions to ∞ takes place at all values of P, Q and δ, except for some special cases, e.g. at $Q_* = 0$, $P_* = -1.5603$, $\delta = 1$ the function $W'(x)$ is limited at all x. If δ and P are positive then the function $W'(x)$ has no zeros at $x > 0$. The same picture is observed at $\delta = -1$, $P > 0$ and sufficiently large Q, as curve 1 in figure 1 testifies. The decrease of Q results in the appearance of a function $W'(x)$ with a two-fold zero (curve 2). With the further decrease of Q zeros part (curve 3), and then a new pair of roots originates (curve 4). Thus we can see that several solutions of boundary-value problems with different values $x_m = x_{m_i}$ and physical parameters R_i and K_i determined by (2.15), respectively, can correspond to one and the same initial-value problem with fixed P and Q. In the case $P > 0$ and $\delta = -1$ the number of such 'related' solutions is even and at $P < 0$ it is odd irrespective of δ. With the decrease of Q to zero the number of 'related' solutions increases infinitely. At the same time, for $Q = 0$ and all values of P from the set $\{-1.5603 < P < 0$ for $\delta = 1$, $P > 0$ for $\delta = -1\}$, the solution is unique and non-oscillating. This irregular transition to the limit $Q \rightarrow 0$ also takes place for other admissible values of P: $P < P_* = -1.5603$ for $\delta = 1$, $P > 0$ for $\delta = -1$, for which there is no solution at all if $Q = 0$. It should be emphasized that the described process of generating the pairs of 'related' solutions does not directly imply the non-uniqueness of solutions for the initial boundary-value problem; nevertheless it is related to this fact, as we shall see further.

All calculations have been performed by the Runge–Kutta–Merson method with automatic choice of step, at the relative error 10^{-4}–10^{-5}. To determine the number of related solutions or the number of $W'(x)$-function zeros for given P, Q, calculations

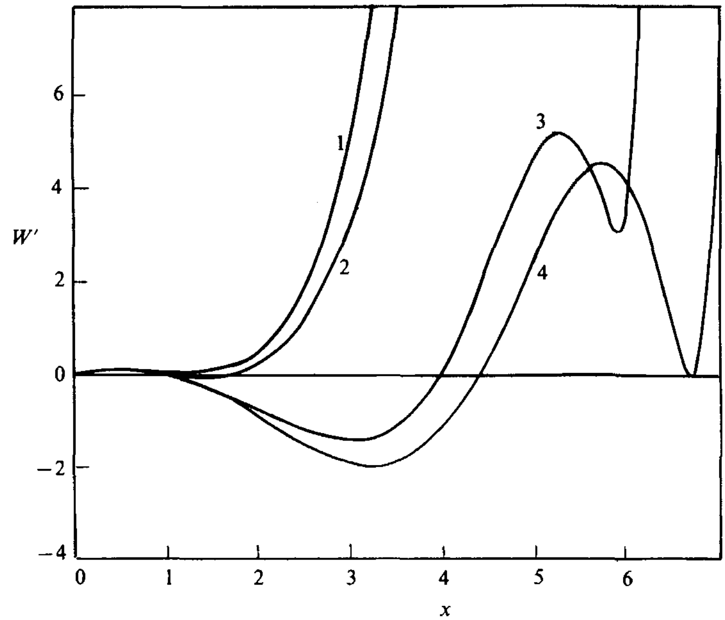

FIGURE 1. Occurrence of 'related' solutions of the initial-value problem at $P = 0.5$, $\delta = -1$. Solutions originate with the decrease of Q. Curve 1 corresponds to $Q = 0.75$, no solutions; curve 2, $Q = 0.677$, double-degenerate solution; curve 3, $Q = 0.32$, two different solutions; curve 4, $Q = 0.277$, new pair of solutions originates.

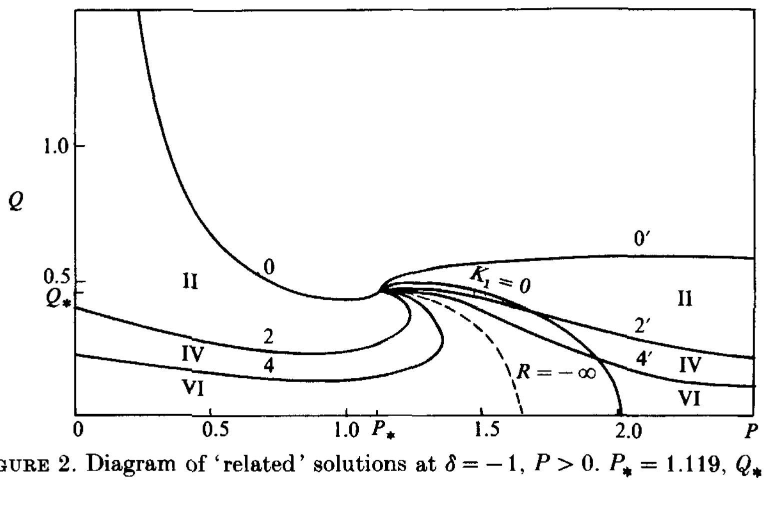

FIGURE 2. Diagram of 'related' solutions at $\delta = -1$, $P > 0$. $P_* = 1.119$, $Q_* = 0.459$.

have been carried out until the values of functions $W(x), \gamma(x)$ become more than 10^{10}, corresponding to their stable growth to infinity. The corresponding value of x_∞ did not exceed 100 for almost all cases considered. Physical parameters R and K were determined in the course of every calculation by the formulae (2.15). Note that by virtue of determining the number $R = Vh/\nu$, $R > 0$ corresponds to suction through the upper porous disk, and $R < 0$ to injection. For $Q > 0$ one needs to consider all values $-\infty < K < \infty$, since the value $K < 0$ can be produced owing to the possible sign change of ω as noted in §3. For the description of all solutions for boundary-value problems one should find all 'related' solutions of every initial-value

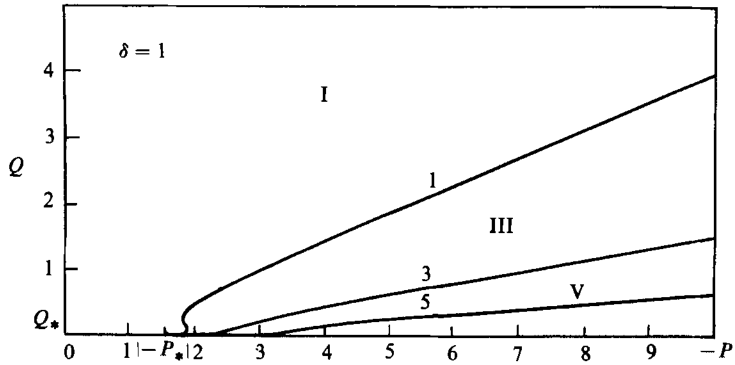

FIGURE 3. Diagram of 'related' solutions at $\delta = 1$, $P < 0$. $P_* = -1.5603$, $Q_* = 0$.

problem. Existence domains of the 'related' solutions on the plane P, Q are shown for the case $\delta = -1$ in figure 2 and for $\delta = 1$ in figure 3. In the region above the curves 0 and 0′ there are no solutions satisfying boundary conditions (2.10). Below these, curves 2 and 2′ up to the curves 4 and 4′, there are four 'related' solutions and so on. All curves of pair production of 'related' solutions meet at the singular point (P_*, Q_*), being a focus to which these curves are spiralling. All $x_{m_i} \to \infty$ on approaching this point. Also, at the dotted curve and the axis $Q = 0$ all $x_{m_i} \to \infty$, except x_{m_1}. Thus, the plane P, Q is divided by the dotted curve in two domains. On this curve as well as on the axis $Q = 0$ all $R_i = -\infty$, except R_1, which remains finite and changes continuously. The values of K_i, except K_1, undergo a discontinuity at the dotted curve. Thereby, regimes with a sign-changing rotation are located to the right of the dotted line. $K_1 \to 0$ when $Q \to 0$, corresponding to the solution of the problem of uniform suction without rotation. K_1 changes sign continuously on a particular curve $(K_1 = 0)$: this corresponds to the bifurcation phenomenon of the rotational regime discussed in §3. The results of figure 4 are obtained if Q ($K = 0$ and cannot serve as the rotation characteristic) is assumed as the measure of the rotation rate. The critical value $R_{\text{crit}} = 6.5$ agrees quite well with the estimation of §3. As is seen from figure 4, the excitation is mild, indicative of the stability of a new regime and instability of an initial one (Arnol'd 1978).

In the case $\delta = 1$ the situation is essentially similar to that for $\delta = -1$. Here there is also a point (P_*, Q_*) see figure 3, where $R = -\infty$ $(P_* = -1.5603, Q_* = 0)$. The ray $Q = 0, |P| \geqslant |P_*|$ is a particular line, on which $R = -\infty$. The difference is that solutions exist only at $P < 0$. Since all solutions can be obtained from the solutions with $\delta = -1$ by extrapolation through the point $P = -\infty$ then there is an odd number of them between these curves and at $P < 0$ at least one solution exists. In region I above curve 1 there is one solution; in region III between curves 1 and 3 there are three solutions, etc. All these regions are subtended into essentially the particular point (P_*, Q_*). The solution with $Q = 0$ and $0 > P > P_*$ corresponds to pure injection. Note that for injection the rotation bifurcation is not observed, in agreement with the analysis of §3. Information on 'related' solutions of the initial-value problem allows the classification of these solutions of the initial boundary-value problem. For injection the regime map in terms of the physical variables R and K is shown in figure 5. There are one, three, five, etc. solutions in regions I, III, V, etc. respectively. These solutions differ topologically both with respect to the number of cells and the presence of counter-rotation. In region I the solution has one or two

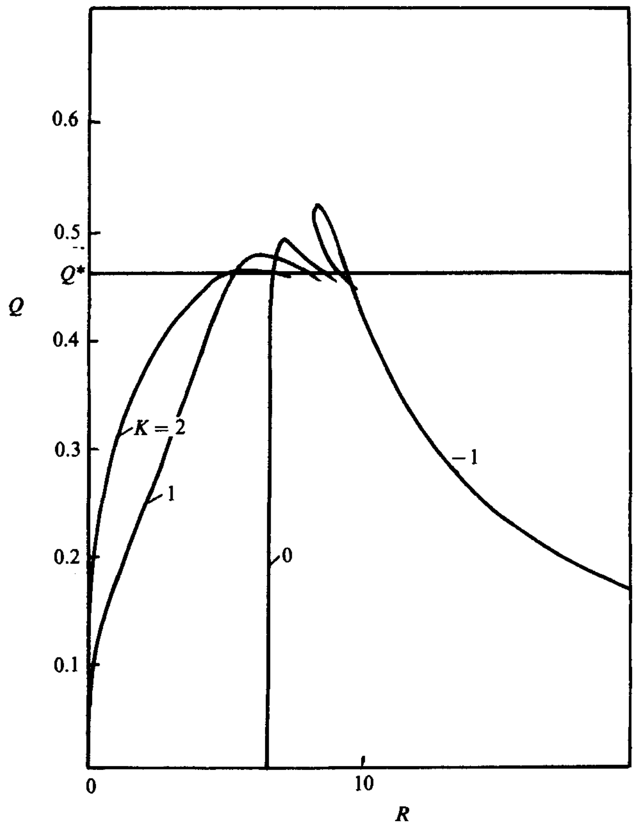

FIGURE 4. Isolines $K = \text{const}$ for unicellular regimes on the plane of parameters R, Q, $\delta = -1$. Isolines with $K > 0$ originate from the point $(0, 0)$ and those with $K < 0$ from the point $(\infty, 0)$. The curve $K = 0$ is a bifurcation autorotation curve. Bifurcation takes place at $R_{\text{crit}} = 6.5$. With the increase of R all isolines tend to the asymptote $Q = Q_*$ (for the solution with $K < 0$ there is a second asymptote $Q = 0$).

cells and rotation of constant sign. In region III, apart from the above-mentioned solution, there are two more. Both have a sign-changing rotation, but the first solution is unicellular and the second one is bicellular. In region V two more solutions are added, both characterized by sign-changing rotation. Additional solutions are not related to the initial stable solution by the bifurcational curve and they are isolated.

It is of interest to compare the results of the non-viscous analysis (§3) with numerical calculations at large Reynolds numbers. It should be pointed out that in practice within the frames of the calculation method proposed it is only possible to obtain large Reynolds numbers ($\sim 10^4$–10^5) in the case of injection. For suction, with the increase of R at given K the values $(P, Q) \rightarrow (P_*, Q_*)$ asymptotically spiralling to the limiting point. It increases significantly the requirements of the calculation accuracy, and does not allow solutions for large values of R to be obtained with the available computer accuracy. On the other hand, as it has been pointed out in §3, at suction non-classical boundary layers arise, reflected in fact in these indicated difficulties of numerical calculation.

A possible qualitative picture of the solution behaviour for $R \rightarrow \infty$ ($\nu \rightarrow 0$) in the case of injection has been presented in the previous section, where it was stated that

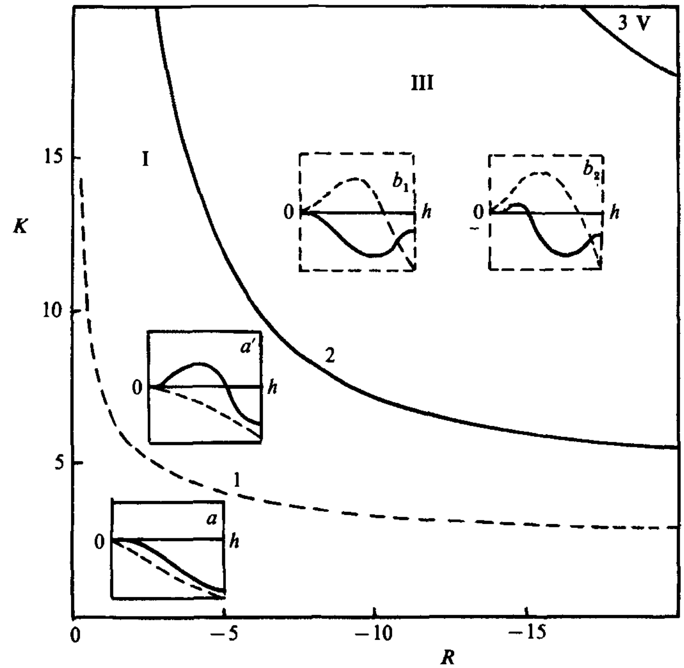

FIGURE 5. Diagram of flow regimes at injection. In the figure the insets show the characteristic features of v_z (——) and ω (----) for each solution of regions I and III. The stable solutions are denoted by an unbroken frame and the unstable solutions by a dotted frame. Below dotted line 1 the solution has one cell, above it, two cells. Curve 2 is a boundary of region III. Curve 3 is a boundary of region V.

additional solutions are possible only for $K > \frac{5}{2}\pi$. At first glance this fact is in contradiction with the presence of the type-b_1 solutions in region III in figure 5. The present solutions have a maximum velocity v_z inside the flow regime that is not true for (3.10). Numerical calculations show that with the increase of R, internal motion is enhanced to a larger degree than the flow near the boundary $z = h$, so that in the limit the solution becomes close to an 'eigen' one corresponding to (3.6) at $k \rightarrow \pi$. Therefore solutions of type b have no non-viscous limit. Possibly, this explains the difficulties in numerical calculations, when Reynolds number of not more than 50 can be obtained for such solutions, whereas the Reynolds number constructed with respect to the maximum velocity is $\sim 10^5$. The above peculiarities of the flow raise a question of rigorous mathematical analysis of the existence loss of some stationary solutions at $\nu \rightarrow 0$. However, as is shown below, all these solutions are unstable and therefore are of no physical interest.

Solutions arising in region V have non-viscous limits corresponding to composite solutions (3.10), (3.13), (3.14). This is confirmed by the properties of numerical solutions at large values of R. Thus, the quantity $k = v_z(z)/h\omega(z)$ is an adiabatical invariant in the case of small viscosities. This invariant changes abruptly on crossing the internal boundary layer according to the law

$$k_i = -\tfrac{1}{2}k_{i-1}, \quad V < 0,$$

coinciding with (3.15). In this way (3.12), obtained by the method of matched asymptotics, has been numerically confirmed over the entire viscous solution.

Maps of regimes for the flow with suction are presented in figure 6. In region I there

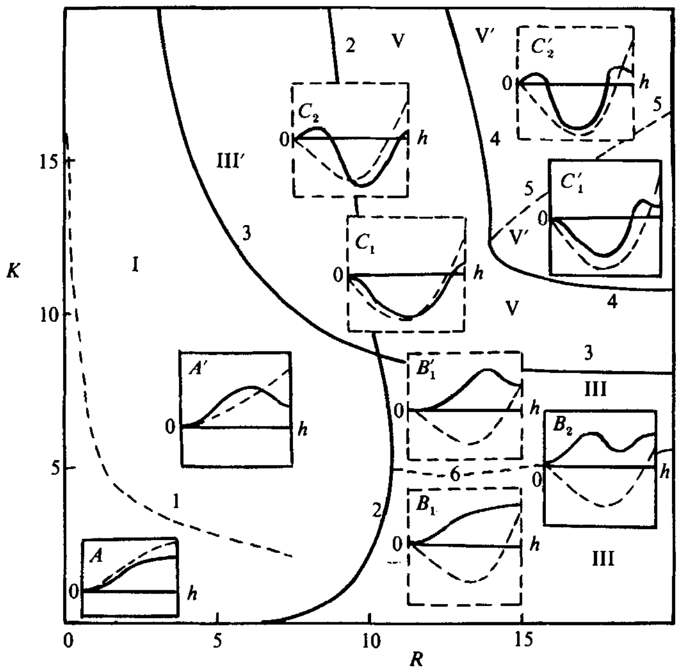

FIGURE 6. Diagram of flow regimes at suction. The insets present the characteristic behaviour of velocities v_z (——) and ω (– – – –). The unbroken frame means that solution is stable and the dotted one that it is unstable. On crossing the dotted curves 1 and 6 the character of the flow corresponding to this solution changes as $A \rightarrow A'$ and $B_1 \rightarrow B_1'$ respectively. On crossing curve 4 in region V′ the character of flow changes so that the unstable solution C_1 transforms into a stable one C_1'. On crossing the boundary formed of the upper part of curve 4 and the dotted curve 5 the solution C_2 transforms to C_2', remaining unstable.

is one stationary solution, in regions III, III′ there are three, in regions V, V′ five, and so on. Curves 2 and 3 are boundaries of regions III and III′ respectively, the intersection region of which is denoted as V–V′. In region I the solution is stable and has one cell with sign-constant rotation. Boundary 2 originates at the point $K = 0$, $R = R_{\text{crit}} = 6.5$, so that the solution in region III exists because of the bifurcation of rotation at this point. One of these solutions is unstable, $B_1 - B_1'$; another is stable, B_2. Both are unicellular with sign-changing rotation. In region III there are two additional unstable solutions, C_1 and C_2, but they are not related to the previous solutions by a bifurcational curve. Both these solutions have a sign-changing rotation. C_1 is two-cellular and C_2 is three-cellular. Thus in the region to the left of curve 2 the unique stable solution A–A' exists. In the region to the right of 2 two metastable solutions, A–A' and B_2, exist. In the region to the right of curve 4 there are three metastable flow regimes, A', B_2 and C_1'. The boundaries 2, 3 and 4 are obtained by the projection on the (R, K)-plane of the three-dimensional bodies shown in figures 7 and 8; moreover the stable flow regime C_1' corresponds to anomalously high lift. As is shown in §3 in the case of suction only three types of solution are asymptotically possible, but in figure 6 we have more of them. The fact is that not all solutions have a non-viscous limit as in the case of injection. Solutions of type C in figure 6 are like these, though it should be noted that some of them are stable at finite R.

As stated in the Introduction, in the case of injection the flow between disks

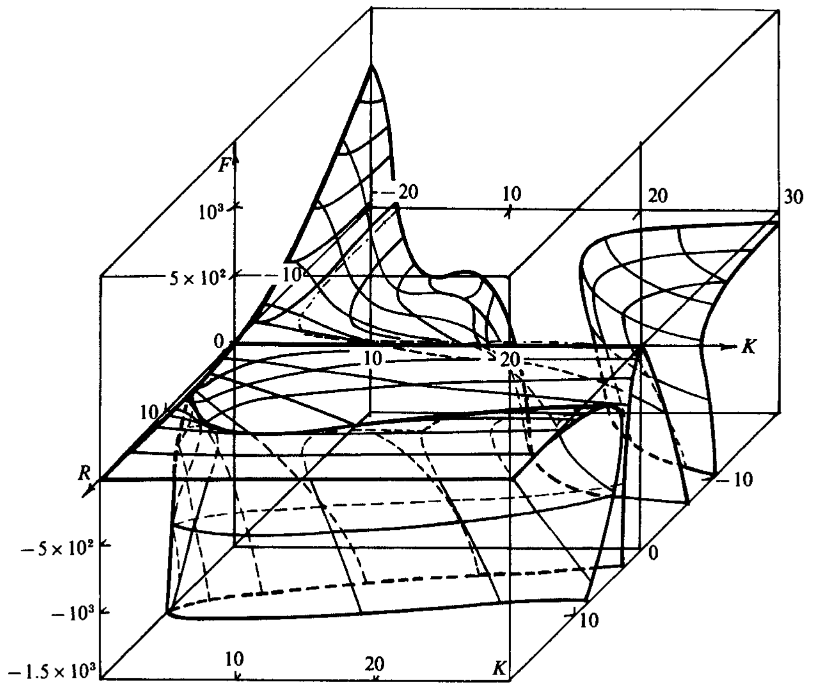

FIGURE 7. Variation of the lift $F(R, K)$ for the family of unicellular solutions for the case of suction ($R > 0$). and one- and two-cellular solutions for the case of injection. At injection (on the background) there is a separate unconnected surface consistent with additional unstable solutions (region V in figure 5). The break corresponds to a particular point $P_*, Q_*, \delta = -1$. In the foreground one can see the deep fold originating because of the bifurcation of rotation at $K = 0$. Isolines $F = \text{const}$ and $R = \text{const}$ are plotted on this surface.

models the flow under a body suspended on an air cushion. It is of interest to observe the effect of the porous-disk (body) rotation on the magnitude of the lifting force. At first glance rotation must decrease the lifting force acting on the porous disk. This is true for unicellular solutions. For multicellular solutions the situation changes sharply. Figure 7 shows the families of unicellular solutions in the form of a surface in three-dimensional space $\mathscr{F}, R, K$, where $\mathscr{F}$ is the lifting force determined according to (2.16). The lifting force F in figure 7 is shown in non-dimensional form by the multiplier $x_m^4\,\delta$ from (2.16). The solution surface is formed by the isolines $F = \text{const}$ and $R = \text{const}$. This surface has two unconnected parts and a rather complicated form. In the foreground, which corresponds to the flow with suction, it is easy to see non-uniqueness of solutions originating because of the rotation bifurcation. This bifurcation forms a deep fold on the surface of solutions and results in the appearance of solutions with large negative values of the lifting force. We can see from the same figure that in the background for another unconnected part of the solution surface, corresponding to injection, a region of values of R and K also exists where the solution is not unique, namely, one can find R and K values at which solutions with a different lifting force are realized. As one would expect, a positive lifting force originates only for the flow with injection ($R < 0$) and decreases with the increase of the twisting parameter K up to zero on the dot-and-dash curve. At large values of K the lifting force is negative. On further increase of K a discontinuity of the solution surface and transition to another branch of solutions are observed. In the (P, Q)-

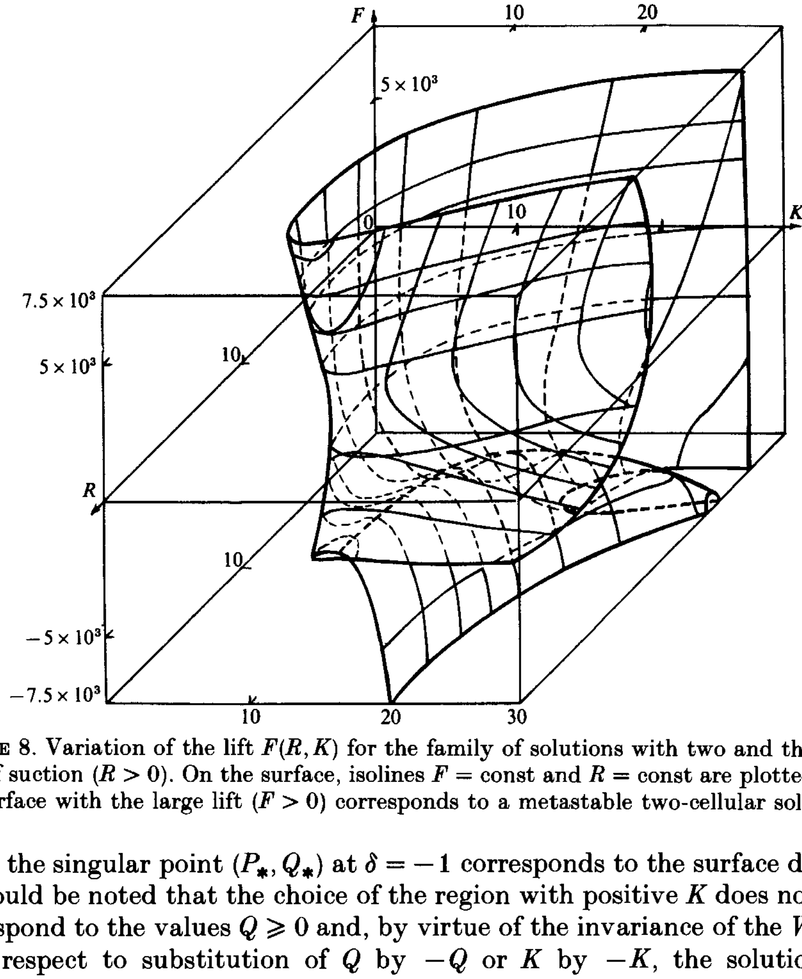

FIGURE 8. Variation of the lift $F(R, K)$ for the family of solutions with two and three cells in the case of suction ($R > 0$). On the surface, isolines $F = \text{const}$ and $R = \text{const}$ are plotted. The front of the surface with the large lift ($F > 0$) corresponds to a metastable two-cellular solution.

plane the singular point (P_*, Q_*) at $\delta = -1$ corresponds to the surface discontinuity. It should be noted that the choice of the region with positive K does not necessarily correspond to the values $Q \geqslant 0$ and, by virtue of the invariance of the $W(x)$ function with respect to substitution of Q by $-Q$ or K by $-K$, the solution surface is transformed symmetrically with respect to the plane $K = 0$ since, for such substitutions, $\gamma(x)$ changes only its sign.

The surface in three-dimensional space F, R, K corresponding to the solutions with two–three cells, is shown in figure 8 for the case of suction. It is of rather complicated shape, with self-crossings being possible. An interesting peculiarity of the solutions considered is that a positive lifting force now originates in the problem of suction, and it is an order of magnitude greater than the value of the lift in the problem of injection with unicellular solutions at the same $|R|$ and $|K|$. The behaviour of additional solutions also turns out to be paradoxical at injection, leading to a very large sinking force. This is illustrated in figure 9, which shows a surface in (F, R, K)-space, corresponding to additional solutions in region III of figure 5. If the above solutions with suction are stable, it would be tempting to use them in practice to obtain high values of the lifting force for a body on an air cushion. It is striking that for this purpose it is necessary to provide suction (!) but not injection.

5. Stability

In the present work the stability problem is considered in the narrow sense of self-similar evolution by solving the nonlinear initial boundary-value problem

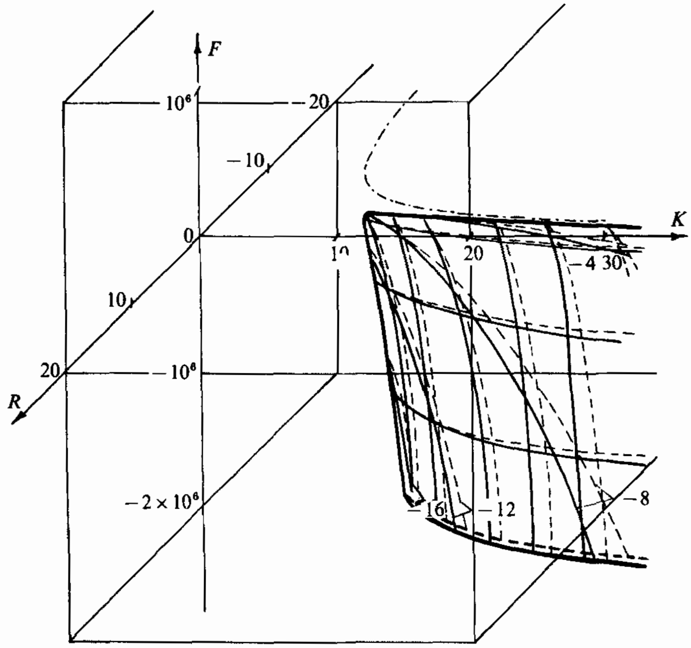

FIGURE 9. Variation of the lift $F(R,K)$ for the family of additional solutions with one or two cells in the case of injection ($R<0$), region III in figure 5. Isolines $F=\text{const}$, $R=\text{const}$, $K=\text{const}$ are plotted. The dot-and-dash line denotes the limiting envelope of the isolines and its projection to the plane $F=0$ (the envelope corresponds to the curve 2 in figure 5).

(2.8)–(2.10). Equations (2.8), (2.9) can be written in non-dimensional form as the following system:

$$\left.\begin{aligned}\frac{\partial\theta}{\partial t}&=\frac{1}{R}\theta''-u\theta'-4\omega\omega',\\ u''&=\theta,\\ \frac{\partial\omega}{\partial t}&=\frac{1}{R}\omega''-u\omega'+u'\omega,\end{aligned}\right\}\tag{5.1}$$

where

$$z\rightarrow\frac{z}{h},\quad u(z)=\frac{v_z}{|V|},\quad \omega(z)\rightarrow\frac{\omega h}{|V|},\quad R=\frac{|V|h}{\nu}.$$

Boundary conditions (2.10) for the function $u(z)$ take the form

$$u(0)=0,\quad u'(0)=0,\quad u(1)=\pm1,\quad u'(1)=0,\tag{5.2}$$

where the plus sign corresponds to suction and the minus sign to injection through the porous disk. In terms of two last conditions (5.2) can be written in the integral form

$$\int_0^1\theta\,\mathrm{d}z=0,\quad \int_0^1 z\theta\,\mathrm{d}z=\mp1.\tag{5.3}$$

For $\omega(z)$ we have the following boundary conditions:

$$\omega(0)=0,\quad \omega(1)=K.\tag{5.4}$$

Initial conditions for the function u,θ,ω should satisfy (5.2)–(5.4) and they are arbitrary in the other respects.

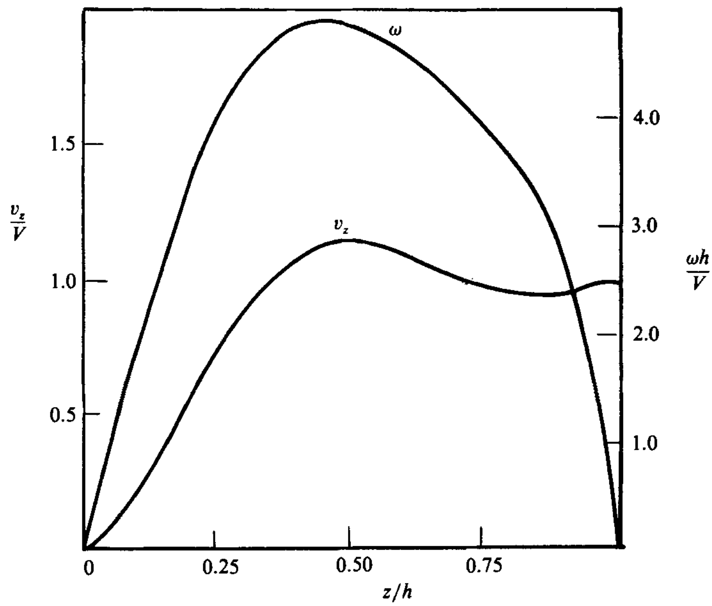

FIGURE 10. Profiles of $v_z(z), \omega(z)$ velocities for the flow between the fixed porous disk ($K = 0$), with uniform suction V, and the impermeable plane at $R = 10$. The solution has been obtained by the evolution of some arbitrary distribution of velocities, which satisfy the boundary conditions and $\omega_0(z) \not\equiv 0$. Setting time is $t_s \approx 10$. Profiles of velocities are given for $t = 15$.

Calculations have been carried out by a finite-difference method of second-order accuracy using an explicit scheme, the integral conditions (5.3) being satisfied with algebraic accuracy using the trapezium formula. These conditions are used for computation of the boundary values $\theta(0)$ and $\theta(1)$ by internal values of the function $\theta(z)$ that allow the use of the boundary condition of the first kind at every executed step for (5.1).

First, the stability of the flow corresponding to spontaneous arising of the fluid rotation between fixed disks has been investigated. As one would expect, the solution without rotation lost stability at suction when the Reynolds number exceeded the critical value $R_{\text{crit}} = 6.5$ and evolved to the stationary solution with rotation found previously. The evolution had a monotonic character up to Reynolds number $R \sim 9$ and it was of oscillating nature when R was larger. The velocity profiles at $R = 10$ are shown in figure 10.

The investigation of the solution stability in the case of injection has shown that only one- or two-cellular flow regimes of a-type (figure 5) are stable and their azimuthal velocity does not change sign in the whole domain $0 \leqslant z \leqslant 1$. These regimes exist at all values of R and K. All additional solutions corresponding to the sign-changing function $\omega(z)$ are unstable. Calculations have proved that the stable solutions tend to the non-viscous limit (3.6), (3.7) or (3.10) with the growth of $|R|$, if $K > \frac{1}{2}\pi$. In the last case, solutions with an internal boundary layer are realized. Thus, in the case of injection the stable solution is unique for any given R and K.

In the case of suction the flow pattern undergoes essential modifications. The first fact that is necessary to point out is the presence of several stable stationary flow regimes (figure 6). So, besides the unicellular A-type solutions with a sign-constant azimuthal velocity, the stable unicellular solutions of B_2 and C_1' types with the sign-changing $\omega(z)$ exist. The presence of several stable stationary solutions is closely

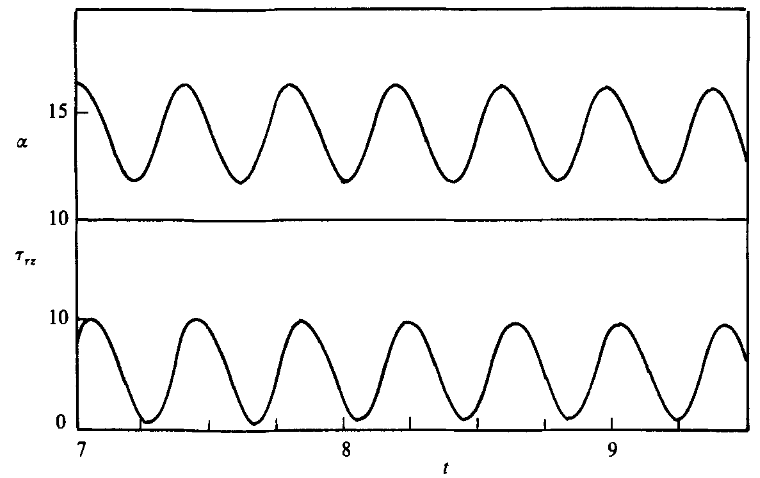

FIGURE 11. Non-dimensional friction $\tau_{rz} = \theta(1,t)/R$ and $\alpha = \theta'(0,t)/R$ as a function of time for the C_1' solution (figure 6) corresponding to high lift and suction. $R = 30, K = 20$. The solution is periodic with period $T = 0.4$. There is a lead in phase shift $\Delta\phi \sim 20°$ between τ_{rz} and α. Setting time for the periodical flow is $t_s \approx 5$.

related to the above-mentioned rotation bifurcation. Curve 2 in figure 6, restricting the existence region of additional stable solutions, starts from the point $K = 0$, $R = R_{\text{crit}} = 6.5$. In the region to the right of curve 2 the solutions are bistable.

Depending on the initial conditions ($\omega_0(z)$ is sign-constant or changes the sign inside the flow region), evolution results in one or other stationary solution. Note that two additional stationary solutions appear to the right of curve 2, but only one of them is stable. Above curve 3 two more new unstable stationary solutions appear. However, one of these solutions, C_1', becomes stable when crossing curve 4, with its topological structure changing. This solution has two cells and sign-changing rotation. It corresponds to large lifting forces acting on a porous rotating disk. Thus, solutions with a large lifting force, discussed in the previous section, turn out to be stable, or more precisely metastable in some range of parameters R, K. The frontal part of the surface with $F > 0$ in figure 8 corresponds to them. In particular, two–three-cellular distributions of velocity $v_z(z)$ with the sign-changing $\omega(z)$ evolve to these solutions. However, stationary solutions with a large lifting force still lose stability with the increase of Reynolds number R (not shown in figure 6, $R^{\text{cr}} > 20$) and a time-periodic solution arises, i.e. a stable limiting cycle originates. Non-dimensional friction $\tau_{rz} = \theta(1,t)/R$ and $\alpha(t) = \theta'(0,t)/R$ are shown as a function of time in figure 11 for the case $R = 30, K = 20$. It is easy to see that the solution is periodic with non-dimensional period $T = 0.4$. With further increase of the time, dependence becomes complicated. Such behaviour in the solution of the boundary-value problem (5.1)–(5.3) resembles qualitatively the solution behaviour of dynamic systems, in particular the Lorentz system. Therefore, it is possible that there is critical Reynolds number $R^{\text{cr}}(K)$ at which the attracting set of unsteady solutions will acquire the features of a strange attractor and the solution will become chaotic. Unfortunately the investigation into the solution behaviour of the non-stationary boundary-value problem (5.1)–(5.3) by the way of evolution becomes still more complicated with the increase of R, and the presence of the additional parameter K complicates the problem yet more. Therefore the emergence of chaos for exact

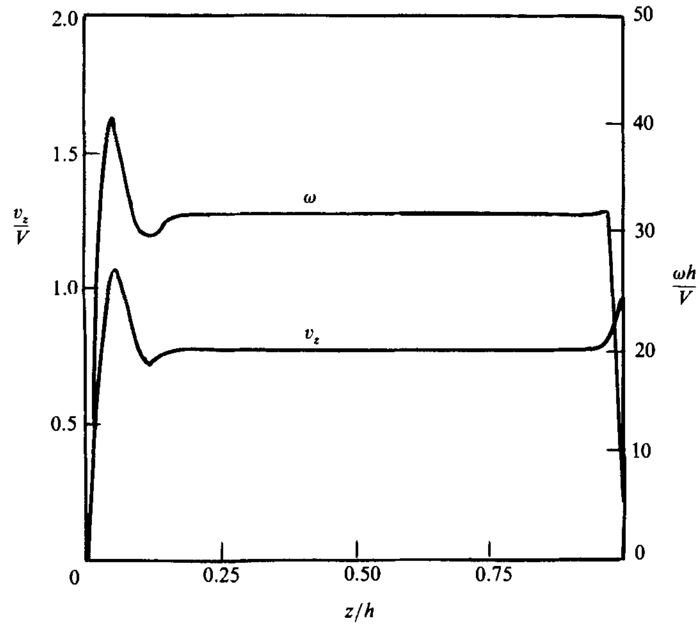

FIGURE 12. Profiles of $v_z(z), \omega(z)$ velocities for the flow with suction at high Reynolds numbers, $R = 100$, $K = 2$. The solution has been obtained by the evolution of some arbitrary initial distribution of velocities satisfying the boundary conditions and $\omega_0(z) \geqslant 0$. The result of the evolution is a solution with $v_z = \text{const}$ and $\omega = \text{const}$ in the core of the flow. It is seen that on crossing non-classical vigorous boundary layers a jump of normal velocity v_z occurs. Setting time is $t_s \approx 10$. Profiles of velocities are given at $t = 13$. $P = 1.106$, $Q = 0.454$, $\alpha = 45.4$, $\delta = -1$.

solutions of the Navier–Stokes equations (the self-similar solutions considered here are of that type) requires additional analytic and numerical investigations.

Another non-trivial property of solutions with suction is the non-classical non-viscous limit at $R \rightarrow \infty$. As has been shown in §3, a non-viscous solution can behave in rather a non-standard manner ((3.19), (3.20)) in the presence of a boundary layer on porous disk at $z = 1$, which is realized only in the case of suction. Not only the no-slip conditions but also the conditions of impermeability (!) are not satisfied for this solution. Computations at large R have shown that this non-viscous limit turns out to be stable in the sense of self-similar evolution. Characteristic velocity profiles are presented in figure 12 at $R = 100, K = 2$. Both stable unicellular solutions A' and B_2 (figure 6) tend to this limit with bistability of the flow preserved also at $R \gg 1$, consistent with (3.20).

The problem of the solution stability has been considered only for the class of arbitrary self-similar disturbances. The general case is rather extensive and should be the subject of additional research.

6. Discussion of results

Some of the results obtained require additional discussion and interpretation. So, the problem is formulated in the infinite region with the velocities v_r and v_ϕ unlimited at infinity. The question arises as to whether the revealed properties of the solutions obtained are due to these infinities. One of these properties is non-uniqueness. If the axisymmetric flow in a finite cylindrical region of radius L is examined then the complete formulation of the boundary-value problem includes representation of the velocity field at $r = L$. In this case only special boundary conditions will lead to the self-similar solutions. Since different boundary conditions meet different self-similar solutions, the non-uniqueness of self-similar solutions does not mean the non-uniqueness of initial boundary-value-problem solutions. From this point of view the non-uniqueness obtained is formally fictitious. However it can have real physical content if we assume that self-similar solutions possess the property of asymptotic stability with respect to variations of boundary conditions at $r = L$. It means that with deviation from the special 'self-similar' boundary conditions at $r = L$, the flow, nevertheless, tends to a self-similar one in its core and details of velocity distribution at $r = L$ are 'forgotten' in some transitional non-self-similar zone. In the whole such behaviour is typical for dissipative systems and it is not impossible for the problem considered here under the condition of the stability of corresponding self-similar regimes. In such a case the space of all possible boundary conditions is divided into a number of subspaces which are subtended by the corresponding self-similar solutions. If this is so, then non-uniqueness of self-similar solutions will correspond to real ambiguity of limiting flow regimes in the region of small r. In this case the role of the boundary conditions at $r = L$ will be reduced to switching the regimes. An experiment is likely to confirm that. In various experimental installations different self-similar conditions of the flow do in fact occur at the same Reynolds number, as has been pointed out in the Introduction.

The non-uniqueness property under discussion is manifested most vividly at the bifurcation of rotation in the case of suction. Spontaneous occurrence of rotation in the purely axisymmetric case seems to be impossible at first glance. This follows directly from (2.2) which is a quasi-linear equation for circulation $\Gamma = rv_\phi$. Since the equation contains no variable Γ, the two-sided maximum principle (Courant & Hilbert 1951) is valid for it: the maximum and minimum are obtained on the region boundary. Thus, if $\Gamma = 0$ on the boundary, the arbitrary initial disturbances will be damped. But this absolutely correct conclusion relates only to the flows 'fixed' on the boundary by the condition $\Gamma = 0$. Hence, the occurrence of self-rotation is possible only owing to a more subtle mechanism: first the flow loses stability with respect to non-axisymmetric disturbances and then a stable secondary regime with non-zero mean rotation develops. This is the way that self-rotation of round jets occurs under certain conditions (Goldshtik, Zhdanova & Shtern 1985).

The motion presented herein is not 'fixed' on its external cylindrical boundary. On the contrary, Kármán's solution (2.5) satisfies the condition of the absence of rotational stress:

$$\tau_{r\phi} = \mu\left[r\frac{\partial}{\partial r}\left(\frac{v_\phi}{r}\right) + \frac{\partial v_r}{r\,\partial\phi}\right] \equiv 0, \tag{6.1}$$

i.e. any external boundary $r = L$ may be considered as 'free' for rotational motion. At boundary condition (6.1), axisymmetric spontaneous arising of rotation is not forbidden and it may principally be observed during an experiment. It would undoubtedly occur in the case of uniform boundary conditions

$$\frac{\partial}{\partial r}\left(\frac{v_r}{r}\right) = 0, \quad \frac{\partial v_z}{\partial r} = 0, \quad r = L, \tag{6.2}$$

which in combination with the condition (6.1) admit the existence of an exact self-similar Kármán solution in the entire region of the flow. However, boundary conditions (6.1), (6.2) are not standard for a hydrodynamic problem and the question of their physical realization in an experiment is still open. It is clear that one of the

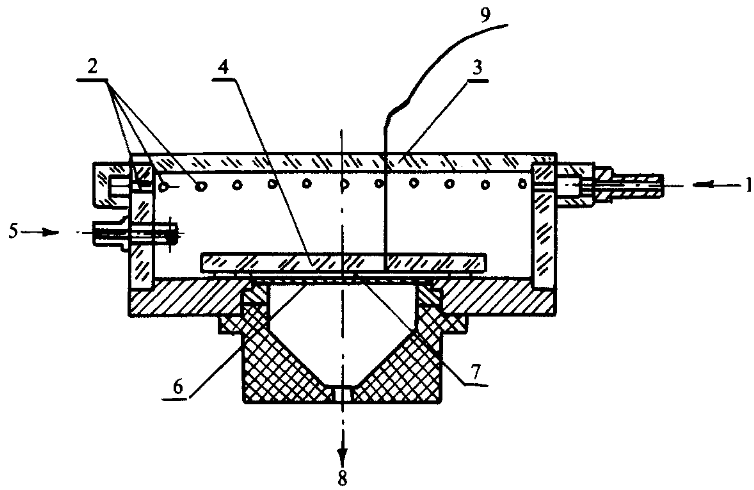

FIGURE 13. Diagram of experimental facility. 1, supply of liquid (distilled water) under pressure; 2, distribution holes; 3, transparent cover; 4, transparent fixed disk; 5, liquid supply to twist the main flow directing tube; 6, metal screen (fixed porous disk); 7, flow region under investigation (transparent disk radius versus clearance $L_t/h = 36$, screen radius versus clearance $L/h = 28$); 8, liquid withdrawal; 9, dye supply through fine capillary for flow visualization.

ways of approximated realization of the condition (6.1) is to set the appropriate external rotation at $r = L$. But then the problem of bifurcation of rotation acquires another sense and must be reformulated. Let distribution $\omega_0(z)$ be given on the boundary $r = L$. Then for $R < R_{\text{crit}} = 6.5$ there is a stationary self-similar solution $\omega_s(z) \equiv 0$. Under these conditions one would expect the emergence of a non-self-similar zone $L_0 < r < L$, where the fast fall of real $\omega(r, z)$ from $\omega_0(z)$ to $\omega(L_0, z) \approx 0$ occurs, so that the rotation in the self-similar core of the flow is practically absent. In the case $R > R_{\text{crit}}, \omega_s(z) \not\equiv 0$, so that rotation should penetrate into the core and attain here a quite definite magnitude depending on R alone, and not on ω_0. If $\omega_0 > \omega_s$ a non-self-similar zone should arise again, where $\omega(r, z)$ decreases fast with the decrease of r. In the case $\omega_0 < \omega_s$ a growth of ω in the non-self-similar zone should take place that is consistent with the tendency of fluid to maintain the circulation Γ, though at $\omega_0 \ll \omega_s$ self-rotation cannot be attained. From the viewpoint of these considerations the bifurcation of rotation indicates the qualitative reconstruction of the flow at $R = R_{\text{crit}}$, which admits experimental verification. To this end we have performed special tests. Figure 13 shows the experimental installation. A rigid metal screen has been used as the porous disk; therefore the no-slip conditions on the porous disk (screen) are not satisfied because of the presence of slipping sections between adjacent wires. To compare the experimental results with the theory, the problem with slipping conditions on porous disk has been calculated:

$$\tau_{rz} = \mu\left(\frac{\partial v_z}{\partial r} + \frac{\partial v_r}{\partial z}\right)\bigg|_{z-h} = 0, \quad \tau_{\phi z} = \mu\left(\frac{\partial v_z}{r\,\partial \phi} + \frac{\partial v_\phi}{\partial z}\right)\bigg|_{z-h} = 0, \tag{6.3}$$

which, in the variables of (2.11), has the form

$$W''(x_m) = 0, \quad \gamma'(x_m) = 0. \tag{6.4}$$

In this case unicellular-solution rotation bifurcation also takes place, shown in the (R, K)-plane in figure 14. The critical Reynolds number is $R^{s}_{\text{crit}} = 1.7$.

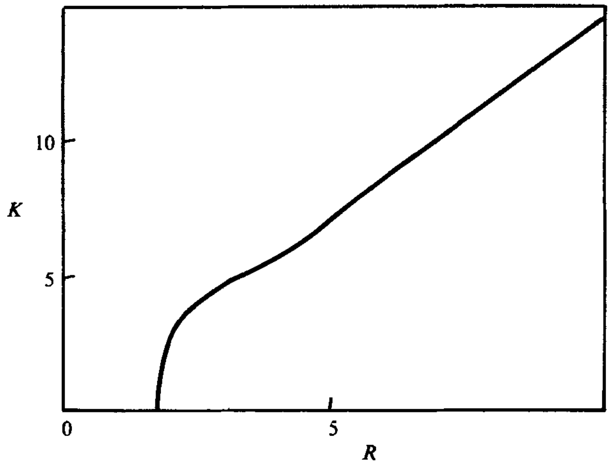

FIGURE 14. Bifurcation of self-rotation branch under the condition of slipping on the porous disk in physical plane R, K.

In our experiments to detect the bifurcation of rotation on the external boundary of disks, a sufficiently large continuously acting twist of inflow was developed, without which fluid rotation in self-similar zone was not observed. With the help of visualization by coloured jets we have found that at $R < 1.7$ in the region adjacent to the axis the flow remains untwisted for all external twists possible in the experiment. At $R \approx 1.7 \pm 0.1$ a flow is reconstructed when rotation arises near the axis, independent of the value of external rotation. Thereby the experiments confirm the existence of the rotation bifurcation and testify to the stability of the rotational flow regime. Thus, the statement about the stability of a secondary regime with rotation relative to self-similar disturbances, which has been obtained numerically by evolution (§5), turns out also to be correct for any disturbances. This allows the hope that solutions with a large lifting force, which are stable with respect to self-similar disturbances, can be realized experimentally, though one should take into account that under conditions of non-uniqueness they can turn out to be metastable with an unknown 'reserve' of stability. One should bear in mind that for the experimental realization of two-cellular flows of type C_1' (figure 6) with large lifting forces the boundary conditions at $r = L$ should correspond to the two-cellular structure of flow shown in figure 15: practically this means the need for powerful peripheral injection with intensive twisting. From this point of view it is quite natural that large lifting forces arise in the case of suction with counter-rotation and it is extremely probable that suction stabilized the flow with a high-pressure zone under the disk. It would be of interest to verify experimentally these suggestions.

7. Conclusion

Thus, non-uniqueness and complex dependence on parameters of the exact self-similar solutions of the Navier–Stokes equations for incompressible fluid flow between a rotating porous disk and an impermeable plane have been found. This non-uniqueness is manifested most vividly in the bifurcation of rotation for the flow between a fixed disk and a plane at sufficiently intensive suction. The other unexpected effect is an anomalously large increase of lifting force at some velocities of the disk rotation and fluid suction, and the flow regimes realized are stable in the

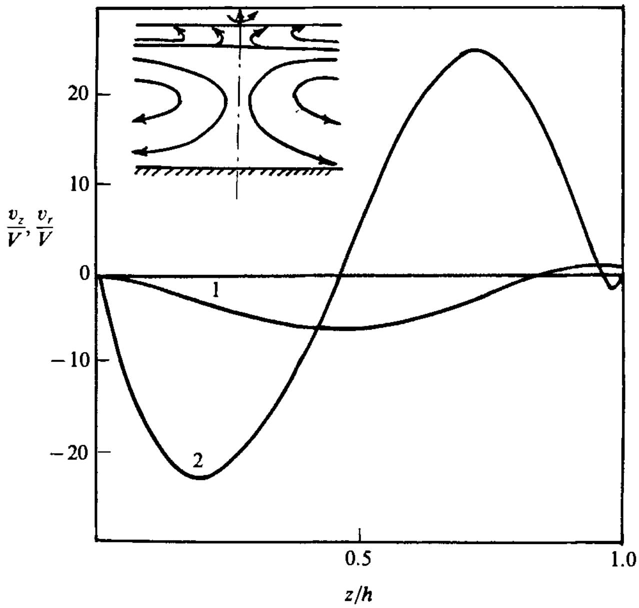

FIGURE 15. Velocity profiles: 1, v_z; 2, v_r, for the solution with suction $R = 20$, $K = 20$, normalized by the suction velocity. The stationary solution obtained by evolution coincides with additional solutions of stationary equations and corresponds to the flow with anomalously high lift (solution C_1'' in figure 6). In the upper left-hand corner streamlines are shown corresponding to this flow. Setting time is $t_s \approx 5$. Velocity diagrams are given for $t = 8$.

sense of self-similar evolution. With the increase of the suction velocity these regimes become self-oscillating. At large suction two stable stationary flow regimes with non-classical boundary layers are realized. In the case of injection there is a unique stable stationary regime. Bifurcation of rotation has been proved experimentally, allowing the hope of obtaining in an experiment the regimes with suction and anomalously large lifting force.

Clearly, all results are obtained for laminar flows. But since the solutions obtained are characterized by volume gradients and internal boundary layers, one can expect that turbulence will be of a free nature. Then the results of the analysis remain valid if constant turbulent viscosity is introduced (Goldshtik 1981). These considerations provide a basis for a more thorough experimental investigation of the motion under consideration with a view to not only its study but possible practical applications as well.

The authors would like to thank A. V. Lebedev for his assistance in the experiments and express their gratitude to referees who contributed much to the improvement of the work.

REFERENCES

ADAMS, M. L. & SZERI, A. Z. 1982 Incompressible flow between finite disks. *Trans. ASME* E: *J. Appl. Mech.* **49**, 1–14.

ARNOL'D, V. I. 1978 *Additional Chapters of Ordinary Differential Equations Theory*. Moscow: Nauka, 304 pp. (in Russian).

BATCHELOR, G. K. 1951 Note on a class of solutions of the Navier–Stokes equations representing steady rotationally-symmetric flow. *Q. J. Mech. Appl. Maths* **4**, 29–41.

BRADY, J. F. & DURLOFSKY, L. 1986 On rotating disk flow: similarity solutions versus finite disks. *J. Fluid Mech.* **175**, 363–394.

COSELSKAYA, N. V. & LUMKIS, E. D. 1980 On the calculation of steady and unsteady flow between infinite rotating disks. In *Applied Problems of Theoretical and Mathematical Physics*, pp. 11–19. Riga (in Russian).

COURANT, R. & HILBERT, D. 1951 *Methods of Mathematical Physics*, Gostehizdat, vol. 2, 620 pp.

DIJKSTRA, D. 1980 On the relation between adjacent inviscid cell type solutions to the rotating-disk equations. *J. Engng Maths* **14**, 133–154.

DIJKSTRA, D. & HEIJST, G. J. F. VAN 1983 The flow between finite rotating disks enclosed by a cylinder. *J. Fluid Mech.* **128**, 123–154.

DORFMANN, L. A. 1966 On the flow of viscous fluid between fixed and blowing on rotating disks. *Izv. Acad. Nauk. SSSR, Fluid Mechanics* **2**, 86–91 (in Russian).

ELCRAT, A. R. 1976 On the radial flow of a viscous fluid between porous disks. *Arch. Rat. Mech. Anal.* **61**, 91–96.

ELCRAT, A. R. 1980 On the flow between a rotating disk and a porous disk. *Arch. Rat. Mech. Anal.* **73**, 63–68.

ELKOUH, A. F. 1968 Laminar flow between rotating porous disks. *J. Engng Mech. Div. ASCE* **94**, 919–929.

ELKOUH, A. F. 1970 Laminar flow between rotating porous disks with equal suction and injection. *J. Méc.* **9**, 429–441.

EVANS, D. J. 1969 The rotationally symmetric flow of a viscous fluid in the presence of an infinite rotating disk with uniform suction. *Q. J. Mech. Appl. Maths* **22**, 467.

GOLDSHTIK, M. A. 1981 *Vortical Flows*. Novosibirsk: Nauka, 366 pp. (in Russian).

GOLDSHTIK, M. A., ZHDANOVA, E. M. & SHTERN, V. N. 1985 The rise rotational motion as a result of hydrodynamical unstability. *Isv. Akad. Nauk. SSSR* **5**, 51–59 (in Russian).

JAWA, M. A. 1971 A numerical study of axially symmetric flow between two rotating infinite porous disks. *Trans. ASME* E: *J. Appl. Mech.* **38**, 100–104.

JUDOVICH, V. I. 1962 On the problem of ideal non-compressible fluid flowing past through the given region. *Dokl. Akad. Nauk. SSSR* **146**, 561–564 (in Russian).

KÁRMÁN, T. VON 1921 Über laminare und turbulente Reibung. *Z. Angew. Math. Mech.* **1**, 232–252.

KREISS, H. O. & PARTER, S. V. 1983 On the swirling flow between rotating coaxial disks: existence and nonuniqueness. *Communs Pure Appl. Maths* **36**, 55–84.

KUIKEN, H. K. 1971 The effect of normal blowing on the flow near a rotating disk of infinite extent. *J. Fluid Mech.* **47**, 789–798.

LIN TSA-TSAO 1958 *Theory of Hydrodynamical Stability*. Moscow: Inostrannaya Literatura, 194 pp.

MELLOR, G. Z., CHAPPLE, P. J. & STOKES, V. K. 1968 On the flow between a rotating and stationary disk. *J. Fluid Mech.* **31**, 95–112.

NARAYANA, C. L. & RUDRAIAH, N. 1972 On the steady flow between a rotating and stationary disk with a uniform suction at the stationary disk. *Z. Angew. Math. Phys.* **23**, 96–104.

NGUYEN, N. D., RIBAULT, J. P. & FLORENT, P. 1975 Multiple solutions for flow between coaxial disks. *J. Fluid Mech.* **68**, 369–388.

OCKENDON, H. 1972 An asymptotic solution for steady flow above an infinite rotating disk with suction. *Q. J. Mech. Appl. Maths* **25**, 291.

PARTER, S. V. 1982 On the swirling flow between rotating coaxial disks: a survey. In *Theory and Applications of Singular Perturbations* (ed. W. Eckhaus & E. M. de Jager). Lecture Notes in Mathematics, vol. 942, pp. 258–280. Springer.

PETROVSKAYA, N. V. 1982 Cross-inflow influence to stationary fluid flow between rotating and fixed porous disk. *J. Prikl. Mech. Techn. Phys.* **5**, 58–61 (in Russian).

RASMUSSEN, H. 1970 Steady viscous flow between two porous disks. *Z. Angew. Math. Phys.* **21**, 187.

RASMUSSEN, H. 1973 A note on the non-unique solutions for the flow between two infinite rotating disks. *Z. Angew. Math. Mech.* **53**, 273.

RECTORIS, K. 1985 *Variational Methods in Mathematical Physics and Technics*. Moscow: Mir, 589 pp.

STUART, J. T. 1954 On the effects of uniform suction on the steady flow due to a rotating disc. *Q. J. Mech. Appl. Maths* **7**, 466.

SZERI, A. L., SCHNEIDER, S. J., LABBE, F. & KAUFMAN, H. N. 1983*a* Flow between rotating disks. Part 1. Basic flow. *J. Fluid Mech.* **134**, 103–131.

SZERI, A. Z., GIRON, A., SCHNEIDER, S. J. & KAUFMAN, H. N. 1983*b* Flow between rotating disks. Part 2. Stability. *J. Fluid Mech.* **134**, 133–154.

WANG, C.-Y. 1976 Symmetric viscous flow between rotating porous disks – moderate rotation. *Q. Appl. Maths* **29**, 29–38.

WANG, C.-Y. & WATSON, L. T. 1979 Viscous flow between rotating discs with injection on the porous disk. *Z. Angew. Math. Phys.* **30**, 773–787.

WILSON, L. O. & SCHRYER, N. L. 1978 Flow between a stationary and rotating disk with suction. *J. Fluid Mech.* **85**, 479–496.

ZANDBERGEN, P. J. & DIJKSTRA, D. 1987 Von Kármán swirling flows. *Ann. Rev. Fluid Mech.* **19**, 465–491.